

## CORRELATED RADIO:X-RAY EMISSION IN THE HARD STATES OF GALACTIC MICROQUASARS

M. CHOUDHURY<sup>1</sup>, A. R. RAO, S. V. VADAWALE

Tata Institute of Fundamental Research, Mumbai-400005, India

A. K. JAIN

ISRO Satellite Centre, Bangalore-560017, India

*Received 2002 November 05; Accepted 2003 April 22*

## ABSTRACT

We present results of our study of correlated radio and X-ray emission in two black hole candidates and Galactic microquasars GRS 1915+105 and Cyg X-1 in their steady long term hard states, along with Cyg X-3 (using data obtained from *Rossi X-Ray Timing Explorer* all-sky monitor [*RXTE*-ASM], *Compton Gamma Ray Observatory* Burst and Transient Source Experiment [*CGRO*-BATSE], and Green Bank Interferometer [GBI]). We detect a pivotal behavior in the X-ray spectrum of GRS 1915+105, correlated to the radio emission. Similar to the results obtained for Cyg X-3, the flux of X-rays softer than the pivoting point correlates with the radio emission, while the corresponding harder X-ray flux anti-correlates with both the radio and the softer X-ray emission, in this state. We examine all the previously reported correlations of X-ray properties with the radio emission in Galactic microquasars and argue that these are consistent with a general picture where a spectral pivoting is a common feature in these sources with the shape of the spectrum determining the flux of radio emission, during the hard states. We also detect a general monotonic increase in the radio emission of these sources with the soft X-ray emission spanning about 5 orders of magnitude. We qualitatively explain these findings with a Two Component Advective Flow model where the location of a boundary layer between the thin disk and the Comptonizing region determines the spectral shape and also the amount of outflow.

*Subject headings:* accretion – binaries : close – stars : individual : Cyg X-3, Cyg X-1, GRS 1915+105 – radio continuum : stars – X-rays : binaries

## 1. INTRODUCTION

The (quasi) simultaneous observations of X-ray binaries in the radio and X-ray bands has led to the notion that the presence of radio jets is ubiquitous in sources with black holes or low magnetic field ( $\lesssim 10^9$  G) neutron stars as compact objects (see Fender 2001a; Fender & Kuulkers 2001). Galactic X-ray binaries exhibiting radio jets (outflow of matter in a collimated beam), with both physical as well as temporal (variability) scale roughly at 6 orders of magnitude less than those of quasars, are termed as *microquasars* (Mirabel & Rodriguez 1999).

Although superluminally moving radio jets are detected in several microquasars (Mirabel & Rodriguez 1994; Tinney et al. 1995; Hjellming & Rupen 1995), which are invariably associated with huge radio flares, only recently it has been realized that non-thermal radio emission is a common feature during relatively quiet phases. Fender (2001a,b) made a detailed calculation of the energetics during such quiet phases and argues that the non-thermal emission forms a substantial part (5%–50%) of the energy budget. Compact radio jets are indeed observed in the low-hard state of several microquasars viz. Cyg X-1 (Stirling et al. 2001), GRS 1915+105 (Dhawan et al. 2000), 1E 1740.7-2942 (Mirabel et al. 1992), and GRS 1758-258 (Rodriguez et al. 1992). Further, the spectral analysis of the radio emission from X-ray transient blackhole candidates, GS 2023+38, GRO J0422+32 and GS 1354-64

(Fender 2001a) and two persistent X-ray blackhole candidates GX 339-4 (Corbel et al. 2000) and XTEJ 1550-564 (Corbel et al. 2001) are interpreted to originate from synchrotron emitting, compact conical jets. A comprehensive study of the association between radio and X-ray emission during the quiet phases of these sources is imperative for understanding the physical mechanism connecting the inflow and outflow of matter, *a.k.a.* the disk-jet connection, in such systems.

The Galactic blackhole candidate GX 339-4 exhibits canonical X-ray states typical for such binary systems. In its low-hard state the source shows very strong correlation between radio and both soft and hard X-ray emissions (Corbel et al. 2003), whereas in the high-soft state the radio emission is quenched (Corbel et al. 2000). For Cyg X-1, the archetypical blackhole binary system, Brocksopp et al. (1999) report that the radio flux is loosely correlated with both soft X-ray (2 – 12 keV, all-sky monitor [ASM]) and hard X-ray (20 – 100 keV, Burst and Transient Source Experiment [BATSE]) fluxes in the low-hard state of the source, with the soft (ASM) and hard (BATSE) X-ray flux being significantly correlated. The radio emission is suppressed in the high-soft state of this source. The enigmatic blackhole candidate GRS 1915+105 shows several variability classes, see Belloni et al. (2000) for the various classifications, of which the class  $\chi$  with steady low X-ray flux has the closest association to the canonical low-hard state (Vadawale et al. 2001a). For this source, Rau

<sup>1</sup>For off prints contact M. Choudhury manoju@tifr.res.in

& Greiner (2003) find no correlation between the radio emission and both soft X-ray emission and wide-band (1 - 200 keV) flux, but find an anti-correlation between hard X-ray (20 - 200 keV) flux and the radio emission. They also find that the slope of the hard power law spectrum correlates positively with the radio flux in this  $\chi$  state. Thus, different types of radio and X-ray correlations have been reported for these sources and a clear and consistent picture of radio and X-ray flux correlation in the low-hard state for these black hole candidates is yet to emerge.

Recently, we have carried out a systematic analysis of correlation between radio, soft, and hard X-ray fluxes as well as a study of changes in wide band X-ray spectral behavior with radio flux in the steady quiescent X-ray state for Cyg X-3 (Choudhury et al. 2002, henceforth Paper 1), a suspected black hole candidate with strong radio emission from a jet (Mioduszewski et al 2001; Marti et al. 2001). The X-ray emission of Cyg X-3 quite distinctively shows low and high states (Rajeev et al. 1994; Nakamura et al. 1993), which correspond to hard and soft states (Choudhury & Rao 2002), distinguished by the shape of the X-ray spectra characterized, chiefly but not totally, by the presence (or absence) of multicoloured disk black-body component and the power-law index (albeit with the individual model components more complicated than the canonical X-ray states of classical black hole candidates characterized, chiefly, by Cyg X-1, see, for eg. Tanaka & Lewin 1995). In Paper 1 we reported a strong and significant correlation between the radio and the soft X-ray emission (2 - 12 keV, [*RXTE*-ASM] in the hard state of Cyg X-3, while the hard X-ray (20 - 100 keV, *CGRO*-BATSE) anti-correlates with both the soft X-ray and the radio, the last anti-correlation was first reported by McCollough et al. (1999). The wide-band X-ray spectral analysis of the pointed *RXTE* observations in this hard state of the source at different radio flux levels show a definite pivoting of the spectrum around 12 keV correlated to the radio emission (see Figure 3 and Table 2 of Paper 1). As the interrelationship between radio and X-ray flux reported in Paper 1 has significant implications for connectivity between accretion disk and radio jet, we have explored other black hole candidates, for which similar radio and X-ray data are available, for radio and X-ray flux correlation analysis.

Here we present results of our analysis for the two persistent X-ray binaries, microquasars and black hole candidates, Cyg X-1 and GRS 1915+105 for which quasi-simultaneous radio and X-ray data are available from GBI, *RXTE*-ASM, and *CGRO*-BATSE. We select data during periods when there are no radio flares and the source is bright both in radio and hard X-rays. We examine radio X-ray correlations in such hard states and show that these correlations are similar to those found in the low-hard states of well studied sources like GX 339-4. We complement our analysis of this state by giving a qualitative self consistent picture of the steady X-ray non-flaring states of these sources, along with Cyg X-3 and GX 339-4, using the Two Component Advective Flow (TCAF) model of Chakrabarti (1996).

## 2. DATA AND ANALYSIS

Fender & Kuulkers (2001) have compiled an extensive list of X-ray binaries, both neutron stars and black hole

candidates, for which simultaneous X-ray and radio observations have been made. The Green Bank Interferometer, West Virginia, operated by NRAO, provides data for a number of X-ray sources that were monitored during its several years of operation. Collating these sources with those monitored by *RXTE*-ASM and *CGRO*-BATSE we found two X-ray binaries (black hole candidates) viz. Cyg X-1 and GRS 1915+105, along with Cyg X-3, which are persistent in radio, soft and hard X-ray bands and for which (quasi) simultaneous data from the three observatories are available.

Figure 1 and Figure 2 give the daily averaged light curves of GRS 1915+105 and Cyg X-1, respectively, in the soft X-ray (ASM, *top panel*), hard X-ray (BATSE, *middle panel*) and the radio (2.2 GHz, GBI, *bottom panel*) during the period when all the three instruments were simultaneously monitoring the sources. Analogous to our approach for testing the correlation among the radio, soft and hard X-ray emission from Cyg X-3 (Paper 1), we have used the Spearman Rank Correlation (SRC) test and adapted the method of partial rank correlation to test the influence of the third parameter (Macklin 1982). The SRC coefficient gives the strength of the correlation between two variables and the corresponding D-parameter gives the confidence level, in terms of standard deviation, that the derived correlation is independent of the influence of the third parameter. Here we also give the results of the correlation analysis for data averaged over different time intervals viz., 1, 5 and 10 days as well as correlation between X-ray hardness ratio (ratio of observed BATSE count rate to that of ASM count rate) and radio (ASM count rate is taken as the third parameter) for the duration in which the respective sources were in a relatively long term steady quiescent hard state. Table 1 gives the complete result of the Spearman Rank Correlation (SRC) test for the correlation among 1) the radio, soft X-ray and hard X-ray, and 2) the hardness ratio in X-ray and radio (GBI) for GRS 1915+105 and Cyg X-1 along with Cyg X-3, during the steady quiescent hard state of X-ray emission, for fluxes in different bands averaged over 1, 5 and 10 days.

As in Paper 1 for Cyg X-3, a detailed wide band spectral analysis of GRS 1915+105 has been done using the pointed mode observations by *RXTE* Proportional Counter Array (PCA) and High Energy X-ray Timing Experiment (HEXTE) instruments available in *RXTE* archive during the period of radio monitoring of this source by GBI. For this purpose, two sets of X-ray data in the  $\chi$  (hard) state of the source and corresponding to two extreme values of the radio flux, within the of precincts of this state, have been used for detailed spectral analysis following the method described in Paper 1. These representative observations, corresponding to the extreme behavior of the sources within the precincts of the respective low and hard states, are marked as inverted arrows in Figure 1 and some features of these observations are given in Table 2. Two unfolded spectra for GRS 1915+105 are overlaid on bottom panel of Figure 3 with top panel showing similar spectra for two extreme values of radio flux in the similar state for Cyg X-3 for comparison purpose (from Paper 1).

### 2.1. Cyg X-3

Cyg X-3 is one of the brightest radio sources associated with an X-ray binary. It exhibits radio flares reaching up to 20 Jy in intensity, with a steady emission in the range of 40 – 150 mJy during the quiescent state (Waltman et al. 1995). Table 1 gives the result of the Spearman Rank Correlation test for fluxes averaged over 1, 5 and 10 days, during the radio quiescent state (see Paper 1, Figure 1), also corresponding to X-ray quiescent and hard state. Though the value of the SRC coefficient increases with increasing bin time, it should be noted that the number of degrees of freedom decreases and hence the best correlation result is obtained for one day averaging (as seen by the value of the null hypothesis probability). Hence the correlation time scale is shorter than a day. The X-ray hardness ratio shows a very strong and significant anti-correlation with the radio emission. Interestingly this anti-correlation is stronger and more significant than the anti-correlation of the hard X-ray flux with radio (or soft X-ray). This suggests spectral bending being correlated with the radio emission, amply demonstrated in the top panel of Figure 3 (see also Figure 3 Paper 1). The pivoting of the spectrum around 12 keV, as obtained from pointed *RXTE* observations, explains the anti-correlation between the soft (2 – 10 keV, *RXTE*-ASM) and hard X-ray (20 – 100 keV *CGRO*-BATSE) emission.

We provide the X-ray wide band spectra following the same procedure as adapted in Paper 1 (see also Vadawale et al. 2001a). The X-ray spectra of black hole sources contain a thermal and a non-thermal part, which are conventionally modeled as a disk black body spectrum and a power-law (or cut-off power-law) or more realistic models incorporating Compton scattering from thermal as well as non-thermal electrons (Zdziarski et al. 2001). Since our aim is to make a wide band description of the spectra to understand the broad features, we have adopted an analytically simpler model consisting of a disk black-body and Comptonization from thermal electrons (Sunyaev & Titarchuk 1980 - the CompST model), plus an additional power law component required to fit the spectra in the quiescent and hard state (Choudhury & Rao 2002). For this source the X-ray spectra below 5 keV is dominated by the numerous photoionization emission lines (Paerels et al. 2000) originating in the hot gas, probably from the dense stellar wind of the Wolf-Rayet companion, engulfing the binary system (Nakamura et al. 1993). Therefore the continuum disk blackbody emission, contributing in the energy range below 5 keV is obscured and hence needs more rigorous analysis and better resolved spectra, which is beyond the scope of this paper. Therefore we present the spectra above 5 keV, modeled with the CompST and power law component. Vadawale et al. (2002) have shown that CompST model gives a functionally correct description of the more elaborate numerical codes, although with slightly different parameters. Moreover, such composite models have been used earlier for Cyg X-3 (Rajeev et al. 1994). Table 2 gives the results of the spectral fitting, along with the soft X-ray (ASM), hard X-ray (BATSE) and radio (2.2 & 8.3 GHz, GBI) flux, of two observations corresponding to the extreme behavior of the source within the precincts of the hard state.

In Paper 1, more spectral data were presented that showed a systematic change in the wide band spectrum

correlated with the radio flux. The available spectra showed a pivoting behavior around 12 – 15 keV. This fact, coupled with the strong correlation between the soft X-ray and radio as well as that anti-correlation of the hard X-ray flux with radio (and soft X-ray flux) strongly suggest that the spectral shape governed by a pivoting behavior at around 12 keV is responsible for the observed correlations.

## 2.2. GRS 1915+105

The X-ray binary GRS 1915+105 was first detected in 1992 (Castro-Tirado et al. 1992), and has been observed in the X-ray, radio and infra-red bands since then (see Belloni et al. 2002, for a review). Munro et al. (2001) classify the radio emission into three classes, radio faint, radio steep and radio plateau, and find that radio emission is always present in the hard steady X-ray state. This source is extremely variable in nature and it has been classified into several variability classes (Belloni et al. 2000). The  $\chi$  class is the closest analogue to the canonical low-hard states of Galactic black hole sources (Rao et al. 2000). Belloni et al. (2000) identify three stretches of long duration  $\chi$  classes and two of them ( $\chi_2$  and  $\chi_3$ ) have simultaneous BATSE and GBI observations. These two periods are demarcated by numbers in the top panel of Figure 1, and are used for the correlation analysis. The results of the SRC test, given in Table 1 are similar to that of Cyg X-3. The radio and soft X-ray fluxes are well correlated. The anti-correlation of the hard X-ray flux with both radio and soft X-ray flux is not as strong as in the case of Cyg X-3. The correlation time scale, as can be concluded from the strength of the correlation, is one day or less. The correlation between the X-ray hardness ratio and radio flux again gives results similar to those of Cyg X-3, suggesting a spectral pivoting correlated to the radio emission. Hence, it is evident that the radio X-ray correlation behavior in the steady long term hard state of this source is similar to that of Cyg X-3.

Two unfolded spectra for GRS 1915+105 corresponding to GBI 8.3 GHz fluxes of 17 and 77 mJy respectively are overlaid in the bottom panel of Figure 3. Table 2 gives the details of the soft X-ray (ASM), hard X-ray (BATSE) and radio (2.2 & 8.3 GHz, GBI) flux along with the best fit parameters of the spectral fitting (Vadawale et al. 2001a). It is interesting to note that the wide-band spectra at extreme radio emissions shows a cross-over at higher energies (20 keV) compared to Cyg X-3 and, by association, we suggest that a spectral pivoting occurring at higher energies is responsible for the observed correlations. A possible reason for a weaker anti-correlation between hard X-ray (20 – 100 keV) flux and soft X-ray (2 – 12 keV) flux (and radio) compared to that in Cyg X-3 is that in the case of Cyg X-3 the soft X-ray (ASM) and hard X-ray (BATSE) energy ranges are, correspondingly, below and above the pivot energy of around 12 keV, whereas for GRS 1915+105, the pivot energy is at higher energies of around 20 keV, and the spectrum is relatively harder.

Rau & Greiner (2003) have made a detailed study of all the  $\chi$  state observations of GRS 1915+105 based on the analysis of four years of pointed *RXTE* PCA and HEXTE observations. They find no correlation between radio and soft X-ray flux (1 – 20 keV), however, they find an anti-correlation between radio and hard X-ray (20-100 keV)

flux, and also find that the slope of hard power law spectrum correlates positively with the radio flux in the low hard state of the source with observations during high radio emission showing a softer spectrum. The latter results agree with our findings presented here. Rau & Greiner (2003) also report spectral pivoting occurring between 20 – 30 keV in X-ray spectra in hard state of GRS 1915+105. The results of Rau & Greiner (2003) are consistent with our findings, except that the radio and soft X-ray fluxes are not correlated in their data, whereas we find a good correlation between radio and soft X-ray flux. Our results are based on the ASM data which is not very sensitive to X-rays above 10 keV, whereas Rau & Greiner (2003) use the flux up to 20 keV using a model fit to the joint PCA and HEXTE observations. The lack of correlation between radio:soft X-ray could be due to the spectral pivoting around 20 keV, because of which the soft X-ray flux from *iRXTE* PCA data will comprise of both correlated and anti-correlated fluxes thus weakening or averaging out the correlation.

### 2.3. Cyg X-1

Cyg X-1 (Bowyer 1965) is the first Galactic black hole candidate (Herrero et al. 1995) whose optical counterpart, O9.7Iab super giant HDE 226868, was among the earliest to be identified for an X-ray binary (Bolton 1972; Webster & Murdin 1972). A persistent source in X-ray, radio (Braes & Miley 1971) and optical, it shows a binary modulation with a period of 5.6 days in all the bands (Pooley et al. 1999; Brocksopp et al. 1999). The radio emission is weak, generally around 15 mJy, varying between 10 to 25 mJy in the low-hard X-ray state getting considerably weaker in the high-soft state of X-ray emission (Brocksopp et al. 1999).

Figure 2 gives the combined light curve of Cyg X-1 in the soft X-ray (2 – 12 keV, ASM, *top panel*), hard X-ray (40 – 140 keV, BATSE, *middle panel*) and the radio (2.2 GHz, GBI, *bottom panel*). The region 1 as demarcated in the top panel of the figure denotes the period of the long term low-hard state of the X-ray emission. Since our emphasis is on the study of the long-term correlated radio: X-ray behavior of this source in low-hard state, we consider only this period for the SRC test. The results of the SRC test for Cyg X-1 are given in Table 1. The table shows that pattern of the correlation between X-ray and radio emission for Cyg X-1 seems to be different than for Cyg X-3 and GRS 1915+105. The soft X-ray and radio fluxes are not as well correlated as for the other two sources, specially for 1 day averages, being only 0.29 compared to 0.68 and 0.56 for Cyg X-3 and GRS 1915+105 respectively. Nevertheless, the correlation is significant at the level of about one part in  $10^6$ . The anti-correlation of hard X-ray (40 – 140 keV, BATSE) flux with the soft X-ray (2 – 10 keV) as well as radio (2.2 GHz, GBI) fluxes found for Cyg X-3 and GRS 1915+105 is not present in Cyg X-1. Instead, the SRC test shows that the hard X-ray positively correlates with the both soft X-ray and radio emission. Also the X-ray hardness ratio does not show any correlation with radio flux in the case of Cyg X-1, unlike for Cyg X-3 and GRS 1915+105.

Brocksopp et al. (1999) report a value of the SRC coefficient for soft X-ray:radio flux correlation in low-hard

state of 0.3 for 1 day average, after removing the mean orbital light curve, which is close to 0.29 found by us for the same correlation, without removal of the orbital modulation effects. Brocksopp et al. (1999) point out that loose correlation of radio and soft X-ray fluxes (for their 1 day averages) may be partly due to the possible offset between the radio and X-ray long period ( $\sim 142$  days) light curves. They also give the scatter plot of ASM, BATSE and radio fluxes.

The strength of the SRC between the radio and the both soft and hard X-ray are similar (Table 1), showing moderately strong correlation, whereas the soft and hard X-ray flux show a very strong positive correlation, the SRC coefficient being 0.70 for 1 day averages. Further, ASM and BATSE observations are at different times during the day implying that intra-day variability is relatively weak compared to variability on longer time scales as both fluxes are strongly correlated over longer time scales. Clearly, the similarity between hard X-ray:radio and soft X-ray: radio flux correlation is because of strong correlation between hard and soft X-ray fluxes. As mentioned earlier, the radio emission in Cyg X-1 is quite weak (around 15 mJy) varying between 10 and 25 mJy in the low-hard state. As the GBI observations have an error of nearly 4 mJy, a detailed wide-band spectral analysis for two extreme values of radio flux, for finding the relation between the shape of the X-ray spectra and the radio emission and the pivoting behavior and the pivot energy, as done for Cyg X-3 and GRS 1915+105, is difficult to be carried out for Cyg X-1.

Zdziarski et al. (2002) have shown that the long term variability of the X-ray emission from this source in hard state comprises of two types of spectral variability, one corresponds to the change in the shape of the spectra (with spectral shape pivoting around 80 keV) with change in soft X-ray flux and the other corresponds to the change in total flux, with the spectra simply moving up and down parallel to each other with a constant shape, in the whole X-ray broad band. This may explain the lack of correlation between the X-ray hardness ratio and the radio flux as well as the comparative weakness of the strength of the SRC correlation between ASM and radio flux. Zdziarski et al. (2002) have analyzed the various correlations among the fluxes of the three energy channels of ASM (1.5 – 3, 3 – 5 and 5 – 12 keV) along with the 20 – 100 keV and 100 – 300 keV flux of BATSE and the corresponding specific spectral index of these bands. They conclusively show that in the low-hard state of the X-ray emission, over long periods, the change in the spectral shape occurs with a pivoting around 50 – 90 keV. This explains that the BATSE flux, being dominated by the lower energy photons is very strongly correlated to the ASM flux. The lack of anti-correlation between the X-ray flux hardness ratio and the radio emission may also be explained by this fact, as the lower energy of the BATSE flux, below the pivot point, is correlated to the radio emission along with the ASM flux.

## 3. DISCUSSION

### 3.1. Comparison with earlier results

The results presented in this paper will be discussed along with similar results for GX 339-4 reported by Corbel et al. (2000, 2003). The compact object in GX 339-4 is also believed to be a black hole (Hynes et al. 2003).

Corbel et al. (2000) find that for GX 339-4, the radio flux is strongly correlated with both soft and hard X-ray, covering the range 3-200 keV, in low-hard state, similar to the results obtained by us for Cyg X-1.

If we consider the results of the radio, soft X-ray and hard X-ray correlation analysis for these four sources, at first glance no consistent picture of the correlated variability pattern emerges. However, it is immediately noticeable that Cyg X-3 and GRS 1915+105 have similar overall correlation pattern. For both, the soft X-ray flux is correlated with the radio flux, and the hard X-ray flux is anti-correlated with the both radio and soft X-ray flux. Additionally, the hardness ratio is also strongly anti-correlated with the radio flux. Wide band X-ray spectral analysis in the hard state for both the sources at different radio flux levels suggests pivoting of the spectrum around 10 – 25 keV correlated with the radio emission.

It can also be noticed that correlation among the radio, soft and hard X-ray fluxes for Cyg X-1 and GX 339-4 is similar. Both show a positive correlation among the radio, soft X-ray and hard X-ray fluxes. For Cyg X-1 the hardness ratio is not correlated with radio flux. Further, Zdziarski et al. (2002) find a pivoting of the X-ray spectrum of Cyg X-1 at higher energy of around 50-90 keV. Similarly, the wide band X-ray to gamma-ray spectral analysis of GX 339-4 (Wardzinski et al. 2002) has shown that there is a pivoting in the spectrum at energies  $\sim 300$  keV in the low-hard state of the source.

At this stage it will be worthwhile to note other similarities in the X-ray and radio emission characteristics of Cyg X-3 and GRS 1915+105 *vis a vis* Cyg X-1 and GX 339-4. Most notable are that the first two sources are the strongest and most variable radio sources amongst the Galactic X-ray binaries whereas both Cyg X-1 and GX 339-4 are amongst the comparatively weak and steady radio sources. On the other hand, both Cyg X-1 and GX 339-4 have a very hard X-ray spectrum compared to Cyg X-3 and GRS 1915+105.

Thus both X-ray sources with softer X-ray spectrum have a lower pivot energy and Cyg X-1 with a much harder X-ray spectrum has a much higher pivot energy, indicating that the pivot energy is directly related to spectral shape. The correlation between hard X-ray flux and radio and soft X-ray fluxes observed in Cyg X-1 and GX 339-4 can then be explained because hard X-ray flux (40 – 140 keV for Cyg X-1, 20-200 keV for GX 339-4) is around or below the pivot energy in these two sources and will, therefore, be correlated with the soft X-ray and thereby the radio fluxes. Thus, it is quite evident that X-ray fluxes below and above the pivot energy are anti-correlated for these X-ray sources and the reported differences between radio, soft X-ray and hard X-ray correlation amongst these X-ray sources is an instrumental artifact where the *RXTE*-ASM and *CGRO*-BATSE energy ranges are fixed and the pivot energy varies from source to source. This is supported by finding of Zdziarski et al. (2002) who report an anti-correlation between 1.5 – 3.0 keV and 100 – 300 keV flux and find a very weak correlation between 1.5 – 3.0 keV and 20 – 100 keV flux for Cyg X-1 in the low-hard state. Thus the X-ray – radio behavior of these X-ray sources are consistent in terms of correlation between soft X-ray, hard X-ray and radio emissions reported here.

### 3.2. The X-ray soft state and suppressed radio emission

In the previous sub-section we have shown that the X-ray radio emission characteristics in the hard states of the highly variable sources Cyg X-3 and GRS 1915+105 are similar to those seen in the low-hard states of the well studied black hole sources Cyg X-1 and GX 339-4, once we assume different pivot energy correlated to the radio emission. Here we explore whether the suppressed radio emission seen in the high-soft states of Cyg X-1 (Brockspott et al. 1999) and GX 339-4 (Corbel et al. 2000) are seen in these two sources. We must caution that the identification of various spectral states using monitoring data is fraught with difficulties of flaring emissions which could be quite delayed in the various emission bands.

Corbel et al. (2000) show that with the X-ray state transition from low-hard to high-soft the radio emission evolves from a jet like synchrotron emission to quenched emission in GX 339-4. This state is generally preceded by a low-hard X-ray (with correlated radio emission) and followed by an X-ray off state (with radio off). For a comparative analysis we plot the radio (GBI, 2.2GHz) and soft X-ray (*RXTE*-ASM, 2-12 keV) scatter diagram in Figure 4 for Cyg X-3 (*top panel*), GRS 1915+105 (*middle panel*) & Cyg X-1 (*bottom panel*), for the non flaring states, which include hard as well as soft states. We have attempted to distinguish the high and low states by the soft X-ray flux and denoted them by open and filled symbols, respectively. For Cyg X-3 the major flares are excluded, and in the process we have excluded the (very low) quenched radio emission immediately preceding the major flares. For GRS 1915+105, too, the data for the radio flares are excluded. It is evident that even for these two sources the radio emission is suppressed in the high state, analogous to the canonical high-soft state. Cyg X-3 shows a very systematic behaviour, with the radio positively correlated to the soft X-ray in the hard state, until it transits to the soft state, where the radio emission is negatively correlated to the soft X-ray emission. For GRS 1915+105 the transition into the soft state with suppressed radio emission is not that drastic but definitely pronounced. Cyg X-1 shows a more scattered association between the radio and X-ray emission, but the suppression of the radio emission with higher ASM flux is evident. Hence, it can be comfortably claimed that the suppression of the radio emission with the X-ray state transition is a generally consistent feature of the X-ray binary systems (BHCs), irrespective of their individual spectral characteristics. Therefore a consistent picture of the accretion-ejection picture is emerging from the observational analysis of sources with apparently very diverse behavioural patterns.

### 3.3. A universal correlation and its origin

In the previous two sub-sections we have shown that the four sources, viz. Cyg X-3, GRS 1915+105, Cyg X-1 and GX 339-4, all show a consistent picture of accretion-ejection mechanism, with the radio emission correlated to the X-ray spectral pivoting in the low state and suppression of the radio emission in the high state following the X-ray state transition. The most notable feature, however, is the strong positive correlation between the radio and soft X-ray flux in the hard state of all the sources. This is similar to the correlation reported for GX 339-4 (Hannikainen

et al. 1998; Corbel et al. 2000; Gallo et al. 2002) and V404 Cyg (Gallo et al. 2002)). We explore below whether the observed correlation is an universal phenomena among the Galactic black hole candidate sources.

In Figure 5, we show a scatter plot of the radio flux against the soft X-ray flux for Cyg X-1 (plus sign), Cyg X-3 (filled circles) and GRS 1915+105 (open circles), all in their corresponding low-hard and their analogous states. The data are normalized to a distance of 1 kpc, with the assumed distances of 2 kpc, 8.5 kpc & 12.5 kpc, respectively for the above three sources. For the soft X-ray flux (based on *RXTE*-ASM data) 75 ASM counts  $s^{-1}$  is taken as the observed Crab flux. Individual data points are the average value for a bin size of 5 days. Recently, Gallo et al. (2002) have detected a correlation between the radio flux ( $S_{radio}$ ) and X-ray flux ( $S_X$ ) of the form  $S_{radio} = k S_X^{+0.7}$  for GX 339-4 and V404 Cyg, all the way from the quiescent level to close to high-soft state transition. This relationship is also shown in Figure 5 as a dotted line (for GX 339-4) and dashed line (for V404 Cyg). The extents of the lines correspond to the data used for the fit in Gallo et al. (2002).

The remarkable feature of Figure 5 is that a simple relation seems to hold for all the black hole sources over close to 5 orders of magnitude variation in the luminosity, in the low-hard state. The data points for Cyg X-1 fall just below the correlation found for GX 339-4, whereas, the data points for GRS 1915+105 lie on the line extrapolated from the correlation derived for V404 Cyg. The data points for Cyg X-3 are parallel to those of GRS 1915+105. It should be noted here that Cyg X-3 shows a very strong orbital modulation which is most probably due to the obscuration of the accretion disk by a cocoon of matter surrounding the accretion disk. Hence the ‘true’ X-ray emission from the accretion disk should be larger than the observed one and the data points should move closer to the extrapolated line from GX 339-4 and V404 Cyg. Since Cyg X-3 is suspected to be a micro-blazar (Fender & Kuulkers 2001), it is also quite possible that the radio emission is over-estimated due to strong beaming and Doppler boosting. It is also noteworthy that GRS 1915+105, the most massive stellar mass black hole known, has the highest intrinsic X-ray emission.

Fitting individual data points of the sources with a function of the form  $S_{radio} = k S_X^{+0.7}$  gives the value of the constant term as 54 mJy, 235 mJy and 1376 mJy, respectively for Cyg X-1, GRS 1915+105 and Cyg X-3. These values should be compared to those obtained for GX 339-4 and V404 Cyg, 124 mJy and 254 mJy, respectively. The individual data points, however, are also consistent with a linear relation and the continuous line in the Figure 5 is a linear fit to the combined data of Cyg X-1 and GRS 1915+105.

Although we cannot completely rule out the possibility that the individual correlations of these sources may exist due to processes unrelated to one another, the fact that the data points for sources close to their ‘off’ states (GX 339-4 and V404 Cyg) occupy one extreme of observations while sources with repeated radio flares (Cyg X-3 and GRS 1915+105) occupy the other extreme strongly suggests of a common physical mechanism in operation in all the sources. One natural consequence to be explored

is whether the radio and the X-ray emissions are emitted directly from the same source region. Since there are very strong observational evidences for the radio emission to be of synchrotron origin, it is tempting to assume that the X-ray emission too is emitted by the same process, but at the base of the jet. There are evidences for X-ray synchrotron emission being responsible for the X-ray spectrum of some black hole sources like XTE J1118+480 (Markoff et al. 2001) and part of the spectrum in sources like GRS 1915+105 (Vadawale et al. 2001a). However, for several black hole sources wide-band X-ray spectrum has been extensively studied and the spectral shape is inconsistent with a simple synchrotron emission. Further, the X-ray:radio correlation appears to be valid from ‘off’ state to low-hard and the associated analogous states, and all the way up to the intermediate state, and it is extremely unlikely that the bulk of the X-ray emission is due to synchrotron emission in all these states.

Recently Markoff et al. (2003) have suggested jet synchrotron emission as a possible way to explain the broad-band (including X-ray) features of GX 339-4. To explain the observed correlation, their model predicts that the X-ray emission is mostly due to synchrotron emission (with a power-law spectral shape). Since the wide band hard X-ray/ low energy gamma-ray spectra of black hole sources in their hard states like GX 339-4 (Wardzinski et al. 2002), GRS 1915+105 (Zdziarski et al. 2001), and Cyg X-1 (Zdziarski 2000) require thermal-Compton emission to explain the spectral shape, we explore below alternate models where the X-ray emission is primarily due to accretion disk emission.

### 3.4. X-ray spectral shape as the “driver” of the radio emission

The wide band X-ray spectral shapes of Galactic X-ray binaries with black holes as compact objects show a systematic and predictable behavior, particularly in well studied sources like Cyg X-1 (Zdziarski 2000) and GX 339-4 (Wardzinski et al. 2002), where, in the low-hard state, the spectral energy distribution peaks at  $\sim 100$ – $300$  keV, with the emission being dominated by thermal-Compton emission from a population of hot electrons. For sources which go to the ‘off’ state the X-ray spectrum is quite similar to the low-hard state, but at a very low intensity. In the intermediate state the soft X-ray flux increases and in the high-soft state the spectrum is dominated by thermal emission from the accretion disk. Although it is quite convenient to assume that the mass accretion rate is responsible for such systematic changes, there is no strong evidence for this (see Homan et al. 2001, for a different behaviour of XTE J1550-654). Nevertheless, one can safely conclude that some unspecified ‘accretion parameters’ causally affect the wide band X-ray spectral shape of black hole X-ray binaries.

The evidences presented in this paper strongly suggests that the very same ‘accretion parameters’ must be causally responsible for the radio emission, rather than the amount of soft X-ray emission, provided they account for the suppressed radio emission in the soft state. Such a hypothesis neatly explains the behavior of Cyg X-3, which is quite bright in all the three energy ranges and hence the observational uncertainty is quite low. It can also be noticed

from Table 1 that the most significant correlation for Cyg X-3 is between the radio emission and the ratio of hard X-ray flux to soft X-rays. Though such an explanation is not very clear in other sources, all the available observations are consistent with this. Since the radio emission too shows increasing emission from ‘off’ state to low-hard state (in GX 339-4 and V404 Cyg), correlated behavior in low-hard state (the above two sources and Cyg X-1), and high radio emission in an intermediate state very close to the high state (in GRS 1915+105 and Cyg X-3) and suppressed radio emission in the high state (Cyg X-3, GRS 1915+105, Cyg X-1 & GX 339-4), we speculate that the soft X-ray intensity determines the spectral shape and the accretion disc condition in these sources, which in turn determines the amount of radio emission (in the X-ray quiescent hard state of these sources). The transition of the systems (Cyg X-3 & GRS 1915+105) into flaring state and their corresponding behavior in the radio as well as X-ray bands is an issue not discussed here.

### 3.5. The TCAF model for the X-ray:radio correlation

Though there are models describing the accretion disk emission (Zdziarski 2000) or jet emission (Markoff et al. 2003), there are very few models which self-consistently solve the accretion and ejection phenomena seen in black hole sources. Since our findings suggest a close connection between these two phenomena, we attempt below to qualitatively explain the X-ray radio association using one such model: the Two Component Advective Flow (TCAF) model of Chakrabarti (1996). According to this model, the Compton scattered X-rays in a black hole source originates from a region close to the compact object, confined within the Centrifugal Boundary Layer (CENBOL). The X-ray spectral shape in various ‘states’ of the source essentially depends on the location of the CENBOL and a detailed description can be found in Chakrabarti & Titarchuk (1995) and Ebisawa et al. (1996). At low accretion rates, the CENBOL is far away from the compact object and the X-ray spectrum is dominated by a thermal-Compton spectrum, originating from the high temperature region within the CENBOL. In the transition state, the CENBOL comes closer to the compact object and the CENBOL can sometimes give rise to radial shocks, causing intense quasi-periodic oscillations, as seen in GRS 1915+105. In the high state, the increased accretion rate produces copious photons in the accretion disc which cool the Compton region, giving rise to very intense disk black-body emission along with bulk motion Comptonization (a power-law in hard X-rays with a photon index of  $\sim 2.5$ ). At some critical accretion rates, the state transitions could be oscillatory as seen in GRS 1915+105 (Chakrabarti & Manickam 2000).

The behavior of TCAF disks and the outflow has been studied in detail in Das & Chakrabarti (1998). The outflow rate is found to be a monotonic function of the compression ratio,  $R$ , of the gas at the shock region. In this scenario, at low accretion rates, the CENBOL is far away from the compact object, and a weak shock can form with low compression ratio, giving low and steady outflow. If this outflow gives rise to radio emission, one can expect a relation between the radio emission and the X-ray emission. In this state (off state to low-hard state), an in-

creased accretion rate increases the overall amount of energy available to the Comptonizing region and hence increasing the X-ray emission. The CENBOL location would be pushed inward, increasing the compression ratio (and hence increasing the radio emission) and also can increase the temperature and optical depth of the Comptonizing region, thus giving rise to a pivoting behavior at hard X-rays (50 – 90 keV) as seen in Cyg X-1 and GX 339-4. At increased accretion rate, the CENBOL can come closer to the compact region, giving the spectral and radio properties as seen in GRS 1915+105 and Cyg X-3. For a given accretion rate the compression ratio, after reaching a critical value (with the shock region coming correspondingly closer to the event horizon), causes the source to transit into the high-soft state state, for which the radio emission is progressively suppressed (Chakrabarti 1999). This model qualitatively explains all the observed X-ray spectral and radio properties of Galactic black hole sources presented here.

## 4. SUMMARY AND CONCLUSIONS

A complete understanding of the accretion-ejection physics in Galactic microquasars demands proper interpretation and modeling of all the varied states of X-ray and radio emission, encompassing the various flaring and steady emissions covering all ranges of time scales. In this paper we have taken a first step in this direction by attempting to understand the long term variation of the (non flaring) radio emission associated with the X-ray emission in the steady hard and soft states. We have analyzed the (quasi) simultaneous observations on GRS 1915+105 and Cyg X-1 using the *RXTE*-ASM, *CGRO*-BATSE and GBI data and made a detailed study of correlation between radio and X-ray fluxes. Based on this analysis along with discussion of earlier published results on Galactic microquasars we find that:

- A correlation exists between the soft X-ray and radio emission of GRS 1915+105 based on the data during the long  $\chi$  state (associated to the low-hard state). The hard X-ray emission is anti-correlated with both radio and soft X-rays. There is a spectral pivoting at around 20 keV, correlated with the radio flux.
- Comparing these results with those of Rau & Greiner (2003) who found a strong correlation between radio emission and the X-ray spectral index in the  $\chi$  states, we conclude that the X-ray and radio emission characteristics of GRS 1915+105 are similar to those of Cyg X-3 (Paper 1). The only difference lies in the values of the pivot energy of the X-ray spectra, which is around  $\sim 12$  keV in Cyg X-3 and around  $\sim 20$  keV in GRS 1915+105.
- A three way correlation among soft X-ray, hard X-ray and radio emission has been found in the low-hard state of Cyg X-1, confirming the results of Brocksopp et al. (1999). Comparing this result with those of Zdziarski et al. (2002) who have found that soft X-ray and hard X-ray above 100 keV are anti-correlated and also that there is a spectral pivoting at around 50 – 90 keV, we

conclude that the X-ray:radio behavior of Cyg X-1 is similar to that of Cyg X-3 and GRS 1915+105, but for the fact that the pivoting energy is at a higher value.

- The X-ray:radio properties of Cyg X-1 are quite similar to that of GX 339-4, where a 3-way correlation between soft X-ray, hard X-ray and radio emission has been reported (Corbel et al. 2000, 2003). Though an anti-correlation between soft X-ray/radio with hard X-rays has not been reported in this source, we note that the X-ray spectrum during low-hard state too shows a pivoting behavior at high energies  $\sim 300$  keV (Wardzinski et al. 2002).
- The radio emission is suppressed for Cyg X-1 & GX 339-4 in their high-soft state and similarly for Cyg X-3 and GRS 1915+105 in their high states (with associated softer spectra). Therefore, all these four sources with apparent diverse X-ray and radio properties show very similar behavioural pattern encompassing the long term steady non-flaring state.
- Compiling the soft X-ray and radio observations of the above sources (GRS 1915+105, Cyg X-3, and Cyg X-1) with the published correlation in GX 339-4 and V404 Cyg (Gallo et al. 2002), we find that all the sources show a monotonic increase of radio emission with the soft X-ray emission, spanning a 5 orders of magnitude variation in their intrinsic luminosities. Cyg X-3

deviates from a single relation by about an order of magnitude which can be reconciled if 1) the observed X-ray intensity is an under-estimate because of obscuration and/or 2) the observed radio intensity is an over-estimate because of beaming and Doppler boosting.

- If a common physical phenomena is responsible for such an uniform relation spanning across 'off' state to intermediate state, we argue that both radiations (X-ray and radio) are unlikely to be originating from a single mechanism like synchrotron emission.
- Finally, we invoke a Two Component Advective Flow (TCAF) model (Chakrabarti 1996) to explain the accretion-ejection behaviour in these systems in the steady hard as well as soft states.

#### ACKNOWLEDGEMENTS

This research has made use of data obtained through the HEASARC Online Service, provided by the NASA/GSFC, and the Green Bank Interferometer, a facility of the National Science Foundation operated by the NRAO in support of NASA High Energy Astrophysics Programs. The authors thank the anonymous referee for the extensive and insightful comments. MC and SVV have been partially supported by the Kanwal Rekhi Scholarship for Career Development. AKJ is grateful to P. S. Goel, Director, ISAC and K. Kasturirangan, Chairman, ISRO, for their constant encouragement and support during the course of this work.

#### REFERENCES

- Belloni, T., Klein-Wolt, M., Mendez, M. et al. 2000, *A&A*, 355, 271  
 Belloni, T., Proc. of the 4th Microquasar Workshop, eds. Ph Durouchoux, Y. Fuchs and J. Rodriguez (Center for Space Physics: Kolkata), 293, astro-ph/0208129  
 Bolton, C.T. 1972, *Nature*, 235, 271  
 Bowyer, S., Byram, E.T., Chubb, T.A., et al. 1965, *Sci*, 147, 394  
 Braes, L.L.E. & Miley, G.K. 1971, *Nature*, 232, 246  
 Brocksopp, C., Fender, R.P., Larionov, V., et al. 1999, *MNRAS*, 309, 1063  
 Castro-Tirado, A.J., Brandt, S. & Lund, N. 1992, *IAU Circ.*, 5590  
 Chakrabarti, S.K. 1996, *Phys. Rep.*, 266, 229  
 Chakrabarti, S.K. 1999, *A&A*, 351, 185  
 Chakrabarti, S. K., & Titarchuk, L. G. 1995, *ApJ*, 455, 623  
 Chakrabarti, S. K., & Manickam, S. G. 2000, *ApJ*, 531, L41  
 Choudhury, M., Rao, A.R., Vadawale, S.V., et al. 2002, *A&A*, 383, L35 (Paper 1)  
 Choudhury, M., & Rao, A.R. 2002, *JApA*, 23, 39  
 Corbel, S., Fender, R.P., Tzioumis, A.K., et al. 2000, *A&A*, 359, 251  
 Corbel, S., Kaaret, P., Jain, R.K., et al. 2001, *ApJ*, 554, 43  
 Corbel, S., Nowak, M.A., Fender, R.P., et al. 2003, *A&A*, 400, 1007  
 Das, T. & Chakrabarti, S.K. 1999, *Class & Quant. Gravity*, 16, 3879  
 Dhawan, V., Mirabel, I.F. & Rodriguez, L.F. 2000, *ApJ*, 543, 373  
 Ebisawa, K., Titarchuk, L. & Chakrabarti, S. 1996, *PASJ*, 48, 59  
 Fender, R.P. 2001a, *MNRAS*, 322, 31  
 Fender, R.P. 2001b, *Ap&SS*, 276(suppl.1), 69  
 Fender, R.P. & Kuulkers, E. 2001, *MNRAS*, 324, 923  
 Gallo, E., Fender, R. & Pooley, G. 2002, Proc. of the 4th Microquasar Workshop, eds. Ph Durouchoux, Y. Fuchs and J. Rodriguez (Center for Space Physics: Kolkata), 209, astro-ph/0207551  
 Hannikainen, D. C., Hunstead, R. W., Campbell-Wilson, D. & Sood, R. K. 1998, *A&A*, 337, 460  
 Herrero, A., Kudritzski, R.P., Gabler, R., et al. 1995, *A&A*, 297, 556  
 Hjellming, R.M. & Rupen, M.P. 1995, *Nature*, 375, 464  
 Homan, J., Wijnands, R., van der Klis, M., et al. 2001, *ApJS*, 132, 377  
 Hynes, R. I., Steeghs, D., Casares, J., Charles, P. A., and O'Brien, K. 2003, *ApJ*, 583, L98.  
 Macklin, J.T. 1982, *MNRAS*, 199, 1119  
 Markoff, S., Falcke, H. & Fender, R. 2001, *A&A*, 372, L25  
 Markoff, S., Nowak, M., Corbel, S., et al. 2003, *A&A*, 397, 645  
 Marti, J., Paredes, J.M. & Peracaula M. 2001, *A&A*, 375, 476  
 McCollough, M.L., Robinson, C.R., Zhang, S.N., et al. 1999, *ApJ*, 517, 951  
 Mioduszewski, A.J., Rupen, M.P., Hjellming, R.J., et al. 2001, *ApJ*, 553, 766  
 Mirabel, I.F., Rodriguez, L.F., Cordier, B., et al. 1992, *Nature*, 358, 215  
 Mirabel, I.F. & Rodriguez, L.F. 1994, *Nature*, 371, 46  
 Mirabel, I.F. & Rodriguez, L.F. 1999, *ARA&A*, 37, 409  
 Munro, M.P., Remillard, R.A., Morgan, E.H., et al. 2001, *ApJ*, 556, 515  
 Nakamura, H., Matsuoka, M., Kawai, N., et al. 1993, *MNRAS*, 261, 353  
 Paerels, F., Cottam, J., Sako, M., et al. 2000, *ApJ*, 533, L135  
 Pooley, G. G., Fender, R. P., & Brocksopp, C. 1999, *MNRAS*, 302, L1  
 Rajeev, M.R., Chitnis, V.R., Rao, A.R., et al. 1994, *ApJ*, 424, 376  
 Rao, A. R., Yadav, J. S. & Paul, B. 2000, *ApJ*, 544, 443  
 Rau, A. & Greiner, J. 2003, *A&A*, 397, 711  
 Rodriguez, L.F., Mirabel, I.F. & Marti, J. 1992, *ApJ*, 401, L15  
 Stirling, A.M., Spencer, R.E., de la Force, C.J., et al. 2001, *MNRAS*, 327, 1273  
 Sunyaev, R.A. & Titarchuk, L.G. 1980, *A&A*, 86, 121  
 Tanaka, Y. & Lewin, W.H.G. 1995, *Cambridge Astrophys. Ser. vol. 26, X-Ray Binaries*, eds. W.H.G. Lewin, J. van Paradijs & E.P.J. van den Heuvel (Cambridge Univ. Press), 126  
 Tingay, S.J., Jauncey, D.L., Preston, R.A., et al. 1995, *Nature*, 374, 141  
 Vadawale, S.V., Rao, A.R., Chakrabarti, S. K. 2001a, *A&A*, 372, 793



- Vadawale, S.V., Rao. A.R., Naik, S. 2002, Proc. of the 4th Microquasar Workshop, eds. Ph Durouchoux, Y. Fuchs and J. Rodriguez (Center for Space Physics: Kolkata), 338
- Waltman, E.B., Ghigo, F.D., Johnston, K.J., et al. 1995, AJ, 110, 290
- Wardzinski, G., Zdziarski, A. A., Gierlinski, M., Grove, J. E., Jahoda, K., & Johnson, W. N. 2002, MNRAS, 337, 829
- Webster, B.L. & Murdin, P. 1972, Nature, 235, 37
- Zdziarski, A.A. 2000, in *High Energy Physical Processes and Mechanisms for Emission from Astrophysical Plasmas*, IAU Symp No 195, P.C.H. Martens, S. Tsuruta, and M. A. Weber, eds., 153p.
- Zdziarski, A.A., Grove, E., Poutanen, J., et al. 2001, ApJ, 554, L45
- Zdziarski, A.A., Poutanen, J., Paciesas, W.A., et al. 2002, ApJ, 578, 357

TABLE 1

THE SPEARMAN RANK CORRELATION (SRC) COEFFICIENT, NULL-HYPOTHESIS PROBABILITY AND D-PARAMETER AMONG 1) THE RADIO, SOFT X-RAY AND HARD X-RAY FLUXES AND 2) THE HARDNESS RATIO OF X-RAY (RATIO OF BATSE TO ASM FLUX), THE RADIO AND THE SOFT X-RAY FLUXES, FOR CYG X-3, GRS 1915+105 AND CYG X-1 IN THE LOW-HARD STATE WITH THE OBSERVED FLUXES AVERAGED FOR 1, 5 AND 10 DAYS.

	Cyg X-3			GRS1915+105			Cyg X-1		
	SRC	Null Prob.	D-Par.	SRC	Null Prob.	D-Par.	SRC	Null Prob.	D-Par.
1 day avg. flux	no.	of data points:	532	no.	of data points:	108	no.	of data points:	268
ASM:GBI	0.68	0	15.9	0.61	$3.6 \times 10^{-12}$	6.8	0.29	$1.6 \times 10^{-6}$	1.4
GBI:BATSE	-0.43	$7.2 \times 10^{-26}$	-3.7	-0.27	$4.1 \times 10^{-3}$	-1.8	0.33	$1.6 \times 10^{-1}$	1.4
ASM:BATSE	-0.48	$1.9 \times 10^{-32}$	-6.7	-0.23	$1.8 \times 10^{-2}$	-0.8	0.70	$2.4 \times 10^{-40}$	13.1
RATIO:GBI	-0.65	0	-3.9	-0.62	$4.0 \times 10^{-13}$	-4.1	0.01	$9.3 \times 10^{-1}$	2.5
5 day avg. flux	no.	of data points:	149	no.	of data points:	32	no.	of data points:	65
ASM:GBI	0.76	$9.9 \times 10^{-29}$	8.1	0.71	$6.6 \times 10^{-6}$	4.4	0.53	$6.6 \times 10^{-6}$	2.0
GBI:BATSE	-0.61	$1.3 \times 10^{-16}$	-2.5	-0.33	$6.7 \times 10^{-2}$	-1.3	0.53	$6.5 \times 10^{-6}$	2.0
ASM:BATSE	-0.68	$2.5 \times 10^{-21}$	-5.3	-0.23	$2.2 \times 10^{-1}$	-0.1	0.72	$1.5 \times 10^{-11}$	5.6
RATIO:GBI	-0.71	$3.9 \times 10^{-31}$	-2.0	-0.65	$5.0 \times 10^{-5}$	-1.5	0.03	$8.4 \times 10^{-1}$	1.6
10 days avg. flux	no.	of data points:	75	no.	of data points:	19	no.	of data points:	33
ASM:GBI	0.83	$2.1 \times 10^{-20}$	6.2	0.67	$1.8 \times 10^{-3}$	3.1	0.58	$4.0 \times 10^{-4}$	1.4
GBI:BATSE	-0.72	$4.7 \times 10^{-13}$	-1.5	-0.23	$3.2 \times 10^{-1}$	-0.8	0.61	$1.0 \times 10^{-4}$	2.0
ASM:BATSE	-0.79	$4.1 \times 10^{-17}$	-3.8	-0.13	$6.0 \times 10^{-1}$	0.2	0.72	$2.8 \times 10^{-6}$	3.4
RATIO:GBI	-0.85	$1.9 \times 10^{-22}$	-2.1	-0.58	$9.2 \times 10^{-3}$	-0.5	0.11	$5.5 \times 10^{-1}$	1.4

TABLE 2

THE OBSERVED FLUXES AND X-RAY SPECTRAL PARAMETERS OF CYG X-3 AND GRS 1915+105 DURING TWO POINTED *RXTE* OBSERVATIONS, CORRESPONDING TO THE EXTREME BEHAVIOUR OF THE SOURCES WITHIN THE PRECINCTS OF THE RESPECTIVE LOW-HARD STATES.

Cyg X-3		
MJD	50717	50954
Flux		
ASM (cts s <sup>-1</sup> )	11.11	5.37
BATSE (ph cm <sup>-2</sup> s <sup>-1</sup> )	0.038	0.058
GBI-2.2 GHz (mJy)	115	43
GBI-8.3GHz (mJy)	165	53
Best fit parameters	CompST+powerlaw	
kT <sub>e</sub> (keV)	5.09±0.38	4.87±0.08
Γ <sub>X</sub>	2.55±0.22	2.01±0.04
χ <sub>ν</sub> <sup>2</sup> (d.o.f.)	0.74(86)	1.42(108)
GRS 1915+105		
MJD	50421	50737
Flux		
ASM (cts s <sup>-1</sup> )	38.59	34.96
BATSE (ph cm <sup>-2</sup> s <sup>-1</sup> )	0.140	0.068
GBI-2.2 GHz (mJy) <sup>1</sup>	29	42
GBI-8.3 GHz (mJy) <sup>1</sup>	17	77
1) Best fit parameters	diskBB+CompST(+powerlaw) <sup>2</sup>	
kT <sub>e</sub> (keV)	20.76 <sup>+1.11</sup> <sub>-0.97</sub>	4.89 <sup>+0.09</sup> <sub>-0.08</sub>
kT <sub>i</sub> n(keV)	1.28 <sup>+0.29</sup> <sub>-0.36</sub>	1.99 <sup>+0.05</sup> <sub>-0.04</sub>
Γ <sub>X</sub>	—	2.49±0.01
χ <sub>ν</sub> <sup>2</sup> (d.o.f.)	1.14(121)	1.55(121)

<sup>1</sup>There is no observation on MJD 50421 for GRS 1915+105, we are quoting values for MJD 50422

<sup>2</sup>The powerlaw component is present for MJD 50737, the radio loud χ state

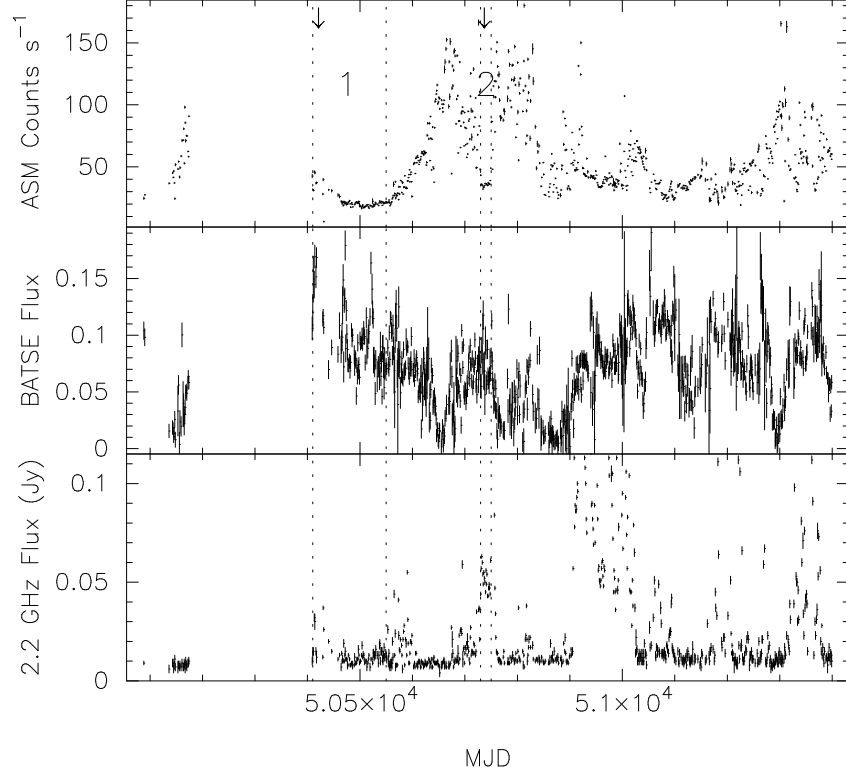


FIG. 1.— The combined simultaneous light curve of GRS 1915+105 in the soft X-ray (2 – 12 keV, ASM, *top panel*), hard X-ray (20 – 100 keV, BATSE, *middle panel*) and the radio (2.2 GHz, GBI, *bottom panel*). The low-hard states, selected for the present analysis (see text), are separated by vertical dashed lines and identified with numbers.

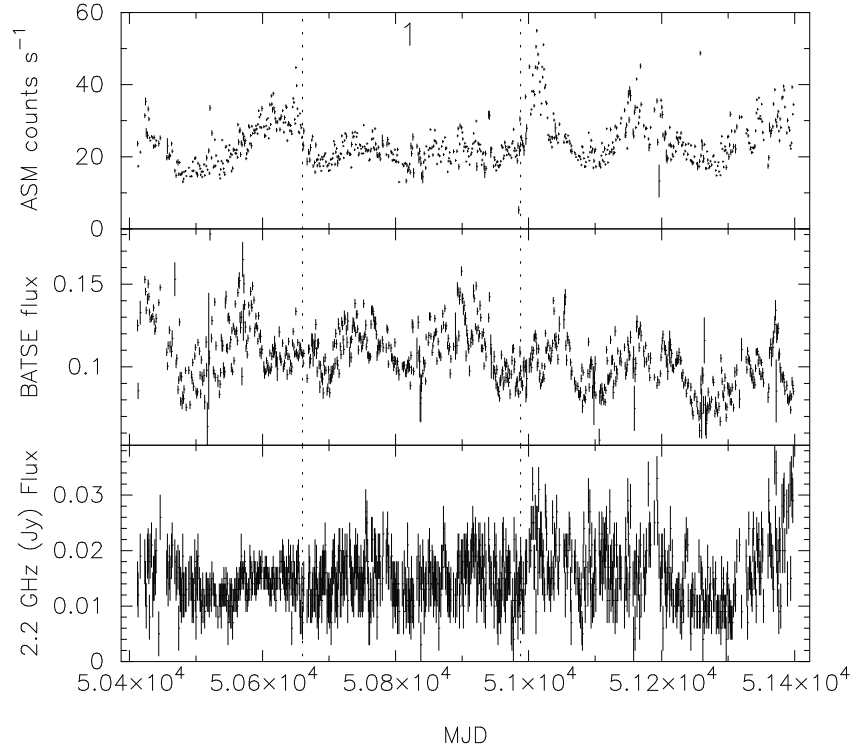


FIG. 2.— The combined simultaneous light curve of Cyg X-1 in the soft X-ray (2 – 12 keV, ASM, *top panel*), hard X-ray (40 – 140 keV, BATSE, *middle panel*) and the radio (2.2 GHz, GBI, *bottom panel*). The low-hard state of the source, selected for the present analysis (see text), is separated by vertical dashed lines and identified with numbers.

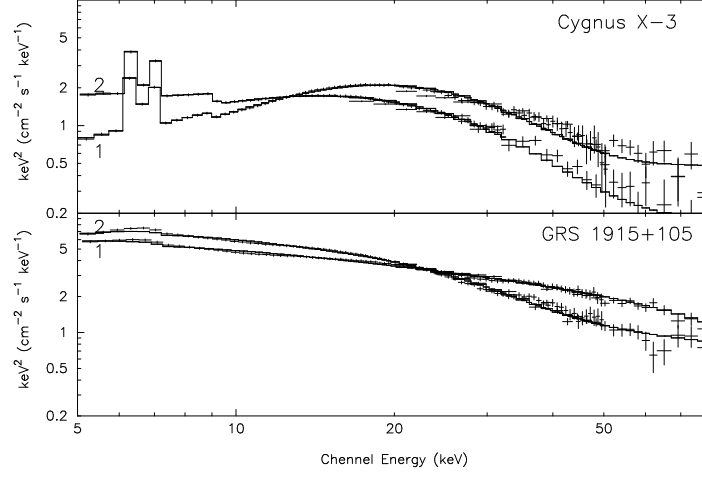


FIG. 3.— *Upper Panel:* Unfolded spectra of Cyg X-3 in the low-hard state (radio quiescent period) on two occasions (1: MJD 50954; 2: MJD 50717). *Lower Panel:* The spectra of GRS 1915+105 in low-hard state on two occasions (1: MJD 50421; 2: MJD 50737).

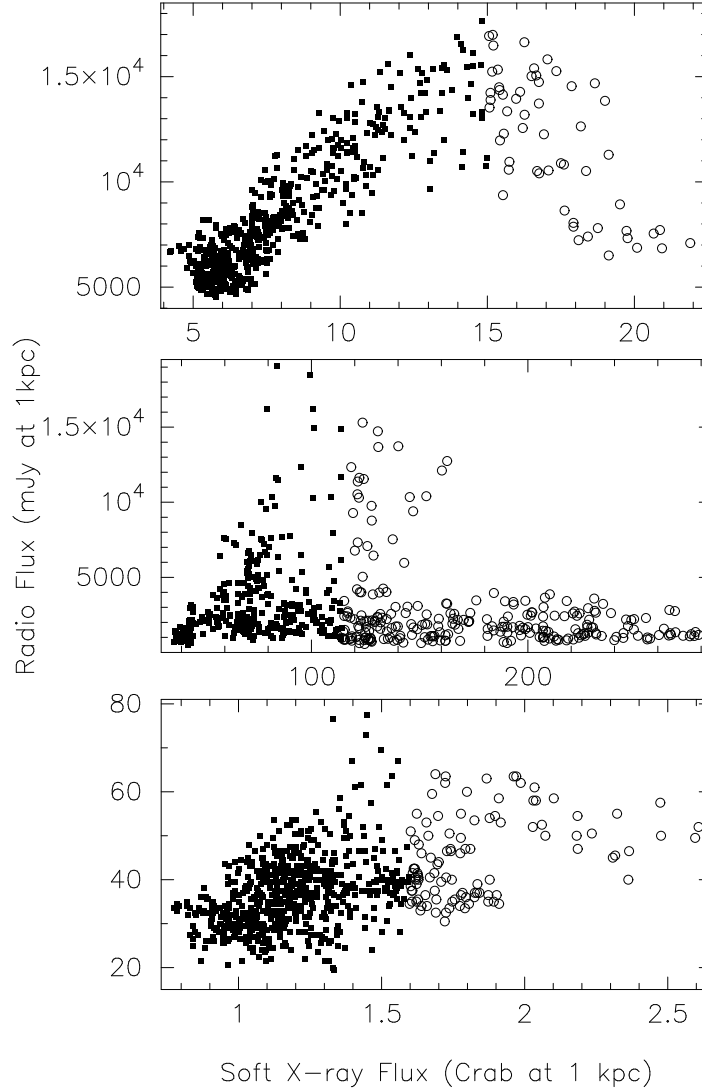


FIG. 4.— The radio (GBI, 2.2GHz) and soft X-ray (*RXTE*-ASM, 2-12 keV) emission scatter diagram of Cyg X-3 (*top panel*), GRS 1915+105 (*middle panel*) and Cyg X-1 (*bottom panel*) for the long-term, steady, hard (*filled squares*) as well as soft (*open circles*) states, after removing the data for the flaring states.

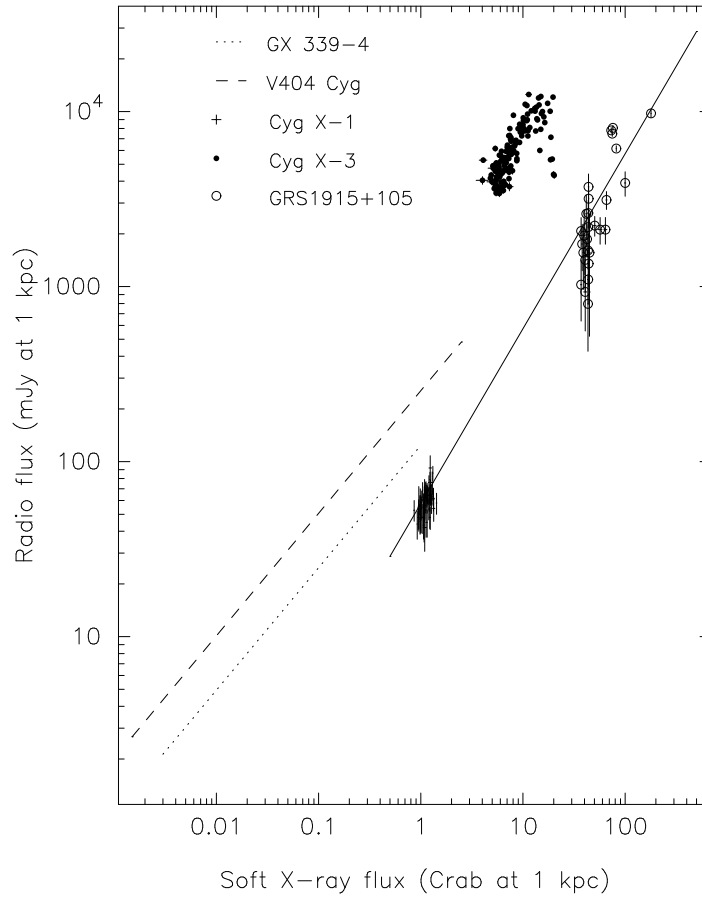


FIG. 5.— A plot of radio flux at 2.2 GHz (based on GBI data) normalized to a distance of 1 kpc against the soft X-ray flux in 2 – 12 keV (based on *RXTE*-ASM data) normalized to Crab at 1 kpc for Cyg X-1, Cyg X-3 and GRS 1915+105, all in their corresponding low-hard states. The data are averaged for 5 days. The power-law fit (with an index of 0.7) reported for GX 339-4 and V404 Cyg by Gallo et al. (2002) are shown as dotted and dashed lines, respectively. The continuous line is a linear fit to the combined data of Cyg X-1 and GRS 1915+105.